Elastin-like recombinamers in collagen-based tubular gels improves their cell-mediated remodelling and viscoelastic properties

D. B. Camasao[1], M. González-Pérez[2], S. Palladino[1], M. Alonso[2], J. C. Rodríguez-Cabello[2], D. Mantovani[1]

[1] Laboratory for Biomaterials and Bioengineering, Canada Research Chair I in Biomaterials and Bioengineering for the Innovation in Surgery, Department of Min-Met-Materials Engineering, Research Center of CHU de Québec, Division of Regenerative Medicine, Laval University, Québec, QC Canada G1V 0A6 [2] BIOFORGE (Group for Advanced Materials and Nanobiotechnology), CIBER-BBN, University of Valladolid, 47011 Valladolid, Spain.

Correspondence: Diego Mantovani, PhD, FBSE, FASM, Laboratory for Biomaterials and Bioengineering, Canada Research Chair I in Biomaterials and Bioengineering for the Innovation in Surgery, Department of Min-Met-Materials Engineering, Research Center of CHU de Québec, Division of Regenerative Medicine, Laval University, Québec, QC Canada G1V 0A6.
E-mail: diego.mantovani@gmn.ulaval.ca

Keywords: elastin-like recombinamers, collagen, soluble elastin, insoluble elastin, cell remodelling, mechanical properties, tubular constructs, vascular tissue engineering

Abstract

Natural polymers are commonly used as scaffolds for vascular tissue engineering. The recognised biological properties of this class of materials are often counterbalanced by their low mechanical performance. In this work, recombinant elastin-like polypeptides (or elastin-like recombinamers, ELR) were mixed with collagen gels and cells to produce cellularized tubular constructs in an attempt to recapitulate the mechanical behavior of the extracellular matrix (ECM). The presence of the elastic protein was found to accelerate construct compaction, cell proliferation and expression of collagen, elastin and fibrillin-1 in a concentration-dependant manner. This compaction is probably the reason for which scaffolds containing 30% of ELR and 70% of collagen (in mass) showed superior mechanical properties. This led to the improvement of 33% in the initial elastic modulus, 64% in the equilibrium elastic modulus, and 37% in the tensile strength without compromising its strain at break, when compared to a pure collagen scaffold. Suggestions for future research include modifications in the crosslinking technology, composition of ELR, polymer concentration, cell seeding density and dynamic stimulation, that have the potential to further improve the mechanical performance of the constructs towards physiological values.

1. Introduction

Natural polymers such as collagen, elastin, chitosan and fibrin are widely investigated for vascular tissue engineering applications due to their excellent biocompatibility (1-6). Collagen is the main extracellular matrix (ECM) protein of blood vessels and therefore shows inherent biological activity, making it even more attractive as scaffolds in this field. In addition, the polymeric chains of the reconstituted collagen retain their ability to self assemble and therefore they can be easily used in biocasting techniques to form tubular gels. Although significant efforts have been dedicated to reproduce the vascular wall composition and structure by combining this protein with vascular cells, their mechanical properties are still far from being comparable to native tissue (7, 8). This motivated the development of composite scaffolds of purely natural polymers aiming to further improve the combination of biological response and mechanical properties. Meeting the mechanical requirements specially in terms of elasticity is the key factor for the success of any substitute in the haemodynamic environment.

Elastin is the second most abundant ECM protein of the native vasculature and the main responsible for its elastic properties. This highly insoluble hydrophobic protein is present in the vessels as large covalently crosslinked network arranged in wavy concentric layers. Elastin is an extremely durable protein and so, it has an extremely low turnover rate *in vivo*. Therefore, different approaches were investigated to induce elastin biosynthesis by cells *in vitro*, such as type of scaffold (9-11), mechanical stimuli (12, 13) and growth factors (14). However, the complex spatial and temporal process to form the functional protein (and the lack of fully comprehension of this process) has prevented those approaches to achieve satisfactory results in terms of elastin content and final elastic properties.

Alternatively, the incorporation of elastin and elastin-derived molecules directly in the fabrication of biomaterials has shown to be an efficient way to overcome the natural low endogenous elastin production (4). Since the complex purification process and insolubility of the mature elastin limit its manipulation and use in biofabrication techniques, soluble elastin forms such as its soluble precursor, tropoelastin or soluble hydrolysed elastin was investigated (15). These forms were showed to maintain their innate assembly, cell interactive capabilities and the elastic behavior for tissue engineering purposes (16). Similarly, recombinant elastin-like polypeptides (or ELR) have recently emerged as a promising alternative due to their tunable composition from modular designs to specifically encoded bioresponsive domains enabling independent tailoring of a range of biomaterials properties (17-19).

The biosynthesis of these ELR became possible in the last few years thanks to the evolution of the biotechnology and genetic engineering which has allowed the production of stable synthetic genes designed to express proteins of interest in heterologous systems (e.g. *Escherichia coli*). In addition to the biocompatibility (introduce this reference: Biocompatibility of two model elastin-like recombinamer-based hydrogels formed through physical or chemical cross-linking for various applications in tissue engineering and regenerative medicine https://doi.org/10.1002/term.2562) and non-immunogenicity of ELR, the biosynthesis procedure assures a precise control over their amino acid sequence and molecular weight (20). Their repetitive backbone based on the hydrophobic and elastomeric region of the natural tropoelastin can be tailored on-demand to be a favorable environment for cell attachment and proliferation by the introduction of cell-binding domains (21-26), to undergo specific covalent and physical crosslinking mechanisms (27-30), and to provide an elasticity comparable to native tissues (31-33).

In this study, the influence of bioactive ELR into tubular collagen gels cellularized with fibroblasts was investigated. This cell type is present in the vascular wall and it is attractive for tissue engineering applications since they are easy to harvest, cultivate and store (34, 35). Furthermore, they are able to secrete matrix proteins *in vitro* in a shorter time frame compared to other vascular cell types (36). These cells were directly mixed with gel solutions containing different proportions of collagen and ELR (0, 3 %, 30 % and 60 % ELR/collagen, % w/w) and poured into tubular molds. Two versions of ELR containing cell-binding domains (RGD) and enzymatically degradable sequences (GTAR) were selected since they have been showed to promote cell attachment, cell proliferation and ECM remodelling (37, 38). In addition, they were functionalized with biocompatible groups that allow an *in-situ* crosslinking reaction under physiological conditions without the need for a catalyst (27, 39). This functionalization is particularly important for the condition which this protein is the major component. Cell-mediated compaction, cell viability and proliferation, ECM expression and viscoelastic properties were evaluated for all conditions after 1, 3, 7 and 14 days of maturation.

2 Materials and Methods

2.1 Cells and cell culture

Neonatal human dermal fibroblasts (HDFn, C0045C, Gibco, Thermo Fisher Scientific, Waltham, MA, USA) were cultured at 37°C in a humidified atmosphere under constant supply of 5% CO_2 in Dulbecco's Modified Eagle Medium (DMEM, Gibco) supplemented with 10% fetal bovine serum (FBS, Gibco), 1% Penicillin-Streptomycin solution (Pen-Strep, Gibco), 5 µg/mL human insulin

(Santa Cruz Biotechnology, Dallas, TX, USA), 2ng/mL Fibroblast Growth Factor-basic (FGFb, Gibco) and 0.5 ng/mL Epidermal Growth Factor (EGF, Invitrogen, Thermo Fisher Scientific). Passages between 7 and 10 were used for all the experiments.

2.2 Preparation of cellularized collagen-ERL constructs

Type I collagen was extracted from rat tail tendons, solubilized in 0.02N acetic acid at a concentration of 4 g/L, sterilized and processed according to a reported protocol (40). Two bioactive ELRs, namely the ELR-RGD and ELR-GTAR, were designed, biosynthesized and decorated with click covalent crosslinkable groups. The ELR-RGD polypeptide, containing six RGD domains, was functionalized with azide groups, while the ELR-GTAR, incorporating four degradable epitopes by the urokinase plasminogen activator (uPA enzyme), was functionalized with cyclooctyne. The two crosslinkable ELR versions were dissolved in PBS at 4 g/L. Gene-synthesis, biosynthesis and purification protocols have been previously described in detail (33, 37, 41). The mechanism of the catalyst-free crosslinking between the azide and cyclooctyne groups was also reported by the same group (27). Modified ELRs were mixed with collagen in four different mass proportions: 0, 3%, 30% and 60% (%w/w). The collagen or ELR-collagen solution was mixed with a neutralizing buffer solution (3.5× DMEM supplemented with 10 mM HEPES and 60 mM NaOH) and a suspension of HDFn in growth factor-free culture medium (DMEM supplemented with 10% of FBS and 1% of Pen-Strep, hereafter referred to as DMEM+) in a proportion of 2:1:1 respectively. The final protein concentration of the gel was 2 g/L (pH 7.2) and cell density of 0.5×10^6 cells/mL. The cellularized collagen solution was poured in a 48-well custom-made plate containing a central polypropylene mandrel (Ø = 3.8 mm). The plate was kept for 1 hour under a sterile biological hood at room temperature (r.t.) to allow the jellification. The tubular gel was gently detached from the wall and medium (DMEM+) was added to fill the well. The plate was incubated at 37°C and 5% CO_2 for 1, 3, 7 or 14 days. Culture medium was changed every day.

2.3 Evaluation of gel compaction and histological staining

The length and outer diameter of the constructs were measured to evaluate gel compaction after 1, 3, 7 and 14 days of culture. A calliper was used to measure the length and a scanning laser interferometer (LaserMike 136, Series 183B, NDC Technologies, Dayton, OH, USA) for the external diameter, similarly to what previously described (42). Since the inner diameter is known and equal to the diameter of the central polypropylene mandrel (Ø = 3.8 mm), the volume of each sample was calculated. Results are expressed as residual volume (%), in other words, the calculated

volume for each sample at each time point was divided by the initial volume of solution added at Day 0 (1 mL). The mean from three different experiments is showed.

Histochemistry (HC) was performed to observe collagen, ELR and cell distribution and compaction. Tubular samples were rinsed in PBS and fixed in 3.7% formaldehyde (Sigma-Aldrich, St Louis, MO, USA) for 1 hour. They were then embedded in paraffin and cut into circumferential cross sections of 5 µm. For HC staining, sections were deparaffinized with toluene, rehydrated with successive washes with ethanol in deionized water (dH_2O) at decreasing concentrations of (100%, 95%, 80%, 70% and 0%) and stained with a modified Verhoeff Van Gieson Elastic Stain Kit (Elastic Stain kit, HT25A, Sigma-Aldrich). Elastic stain solution (hematoxylin, ferric chloride and Weigert's iodine), ferric chloride solution and Van Gieson solution were used to stain elastic fibers (black to black), cell nuclei (blue to black), collagen (red), muscle and other (yellow). Images were obtained by an Olympus BX51 microscope (Olympus Canada Inc., Toronto, ON, Canada).

2.4 Evaluation of cellular metabolic function

At each time point, the culture medium was removed from each well and replaced by 0.8 mL of resazurin solution in DMEM (1:10). The plate was then incubated for four hours at 37°C and 5% CO_2 to allow the reduction of resazurin into the red and highly fluorescent resorufin. Three aliquots from each sample were transferred to a 96-well plate and the fluorescence was measured (λ_{ex} = 560nm; λ_{em} = 590nm) in a multi-well plate spectrophotometer (SpectraMax i3x, Molecular Devices, San Jose, California, USA). Results were normalized over the pure collagen sample (0% ELR) and over Day 1 for each condition. The mean of the three measurements from four different experiments is showed.

2.5 Evaluation of gene expression by HDFn

The expression of different genes of interest by HDFn were assessed by qRT-PCR. RNA was isolated from each sample using TRIzol® Reagent (Thermo Fischer Scientific), according to supplier's instructions. Briefly, the constructs were immersed in TRIzol® reagent and homogenized with tissue grinders. Chloroform was added to separate the organic layer from the aqueous phase containing RNA followed by isopropanol for its precipitation. The RNA pellet obtained after centrifugation was washed with 75% ethanol, resuspended in RNase-free dH_2O and stored at -70°C. The RNA content and purity were determined with Nanodrop (ND-1000 Spectrophotometer, NanoDrop Technologies, Inc., Wilmington, DE, USA). High purity levels were achieved ($A_{260/280}$ >1.8). The QuantiTect® Reverse Transcription Kit (Qiagen Inc., Toronto, ON, Canada) was used to reverse transcribe the isolated RNA into cDNA using a thermal cycler (PTC-200, MJ Research, QC,

Canada), according to manufacturer's guidelines. The real-time PCR was performed using a 7500 Fast Real-Time PCR System (Applied Biosystems, Thermo Fisher Scientific). TaqMan® Gene Expression Assays targeting GAPDH (Hs03929097_g1), type I collagen (col1a1, Hs00164004_m1), elastin (Hs00355783_m1), fibrillin-1 (FBN1, Hs00171191_m1) and Ki-67 (MKI67, Hs01032443_m1) with TAQMAN universal Master mix II with UNG (all purchased from Applied Biosystems) were employed in duplicate for each sample. Finally, the relative quantification of mRNA levels (fold change in relation to the control gene GAPDH and to the condition of pure collagen at Day 1) was calculated using the $2^{-\Delta\Delta Ct}$ method. The mean of the two measurements from three different experiments is showed.

2.6 Evaluation of viscoelastic mechanical properties

The viscoelastic mechanical properties were evaluated by tensile stress relaxation tests using an Instron E1000 (Instron Corporation, Norwood, MA, USA) equipped with a 5N load cell. Ring-shaped samples of approximately 5 mm of length were placed on *ad hoc* made L-shape grips and tested in a PBS bath at 37°C to maintain physiological-like conditions. A pre-strain of 5% was applied to the samples followed by 5 progressive stress-relaxation cycles each consisting of 10% strain ramps (5%/s strain rate) and 10 minutes of relaxation, reaching a final deformation of 55%. The Maxwell-Wiechert model with 2 Maxwell elements was used to fit the data of load and displacement obtained over time using MATLAB (MathWorks, Natick, MA, USA), as previously reported (43). The model is defined by the following equation:

$$\sigma(t) = \varepsilon_0 \cdot E_E + \varepsilon_0 \cdot E_1 \cdot \exp\left(-\frac{t}{\tau_1}\right) + \varepsilon_0 \cdot E_2 \cdot \exp\left(-\frac{t}{\tau_2}\right)$$

where $\sigma(t)$ is the stress at a given time of each relaxation cycle, ε_0 is the applied strain, E_E is the equilibrium elastic modulus, E_i and τ_i (where i = 1 to 2) are the elastic components and relaxation times associated to the Maxwell elements and $\tau_i = \eta_i/E_i$. The sum of E_i and E_E values is defined as the initial (instantaneous) elastic model (E_0). The tensile strength and strain at break are the values of stress and strain at failure respectively of the sample. The mean from four different experiments is showed.

2.7 Statistical analysis

Statistical analyses were performed using GraphPad version 6 (GraphPad software, La Jolla, CA, USA). Comparisons among groups were evaluated by two-way ANOVA with post-hoc Tukey test to correct for multiple comparisons. Significance was retained when $p < 0.05$. Data are expressed as mean ± standard error of the mean (SEM), $n \geq 4$.

3 Results and Discussion

3.1 Effect of ELR on the HDFn-mediated gel compaction

The first immediate effect of adding ELR into the collagen gel was the higher compaction of the samples. Figure 1 shows the residual volume (expressed as percentage with respect to the initial volume) of each condition after 1, 3, 7 and 14 days of maturation.

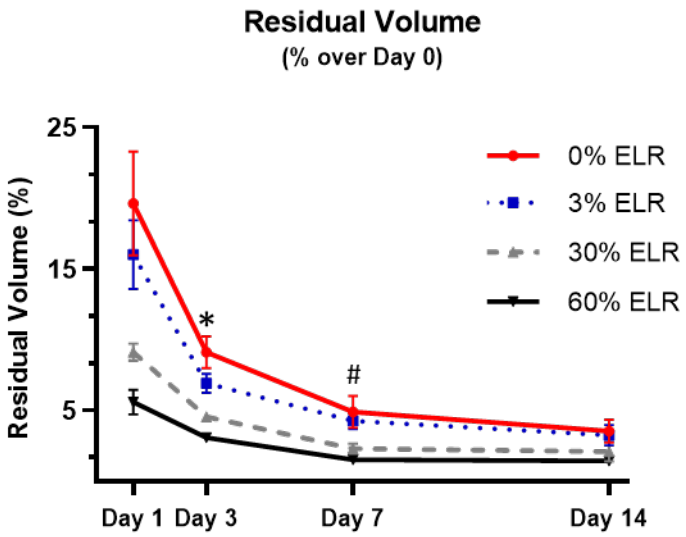

Figure 1: Effect of ELR on HDFn-mediated gel compaction. Time course of construct compaction (residual volume %) at 0% (red dots), 3% (blue squares), 30% (gray triangles) and 60% (black inverted triangles) of ELR in cellularized collagen gel (n=4, *p<0.05 for 60% ELR vs 0% and 3% ELR, # p<0.05 for 60% ELR vs 3% ELR).

An overall time and ELR concentration dependence on the compaction were observed (p<0.05 for time and ELR effect, two-way ANOVA). Already in the first day of maturation, all conditions showed a strong compaction reaching less than 25% of their initial volume (V_0 = 1mL). The presence of ELR resulted in a more pronounced compaction achieving 9.1 ± 0.6% and 5.6 ± 0.9% of the initial volume for the conditions of 30% and 60% of ELR respectively at this time point. The compaction continued for the following days maintaining the trend of highest amount of ELR showing the lowest residual volume. During the second week, the compaction rate decreased for all conditions resulting in constructs with final volume ranging from 1.5-3.5%. The data suggest that a plateau was reached for the conditions of 30% and 60% ELR while for the other conditions

(0% and 3% ELR) it is close to stabilize. This means that cells and the molecules of collagen and ELR are achieving a more pack organization during maturation.

Histological images (Figure 2) confirm the compaction by the decreasing in the cross-sectional thickness and higher intensity of the dye color with time and with the amount of ELR present in the gel. The samples containing higher amounts of ELR (i.e. 30% and 60%) showed a darker color (dark purple) since elastic components were stained in black while the samples containing no or 3% of ELR were predominantly pinky stained. According to the magnified images of Day 1 (first row of Figure 2), the condition of 30% ELR showed a more homogeneous distribution of the ELR whether the condition of 60% ELR showed several spots of ELR aggregation (dark spots). This trend is also observable in the magnification of Day 14 (last row of Figure 2), leading even to the emergence of discontinuous phases.

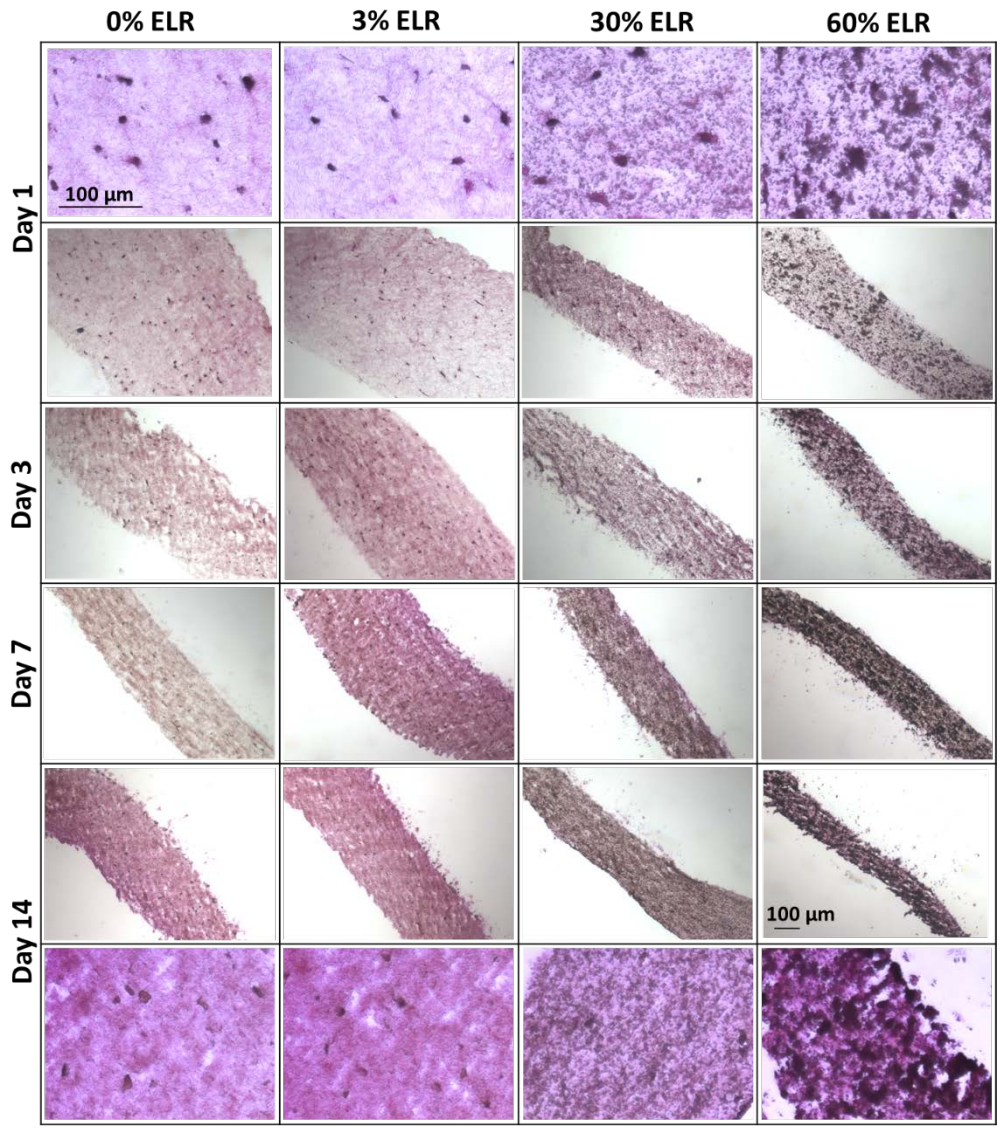

Figure 2: Histological characterization by elastic stain kit of the transversal sections of tubular constructs. Each column shows one condition (0%, 3%, 30% and 60% of ELR in cellularized collagen gel) and the rows different time points. For Day 1 and Day 14, images of higher magnification were added. Elastic components were stained in black to black, nuclei in blue to black, collagen in red, muscle and other in yellow.

De Torre, I. G. et al (2014) studied the mechanisms governing the nanogel formation of the referable ELR solutions at 4°C and 37°C (above and below the transition temperature, pH 7.1). While at 4°C, nanogels showed a linear structure, at 37°C it becomes globular and some aggregation was observed. In the later configuration, the chains experience a high number of intra- and intermolecular hydrophobic contacts resulting in a more solid continuous phase. In this

work, gels were kept under room temperature for 1 hour, and then transferred to a biological incubator at 37°C during the whole period of maturation. The observed aggregations of ELR (present in different proportions mainly in the condition of 30% and 60% ELR) can explain the difference in the residual volume among the conditions of this work, since the decrease of the volume can be related to the lower water content from the intra- and intermolecular hydrophobic interactions of globular ELR nanogels.

Cells are believed to be the main responsible for the time-dependency of the observed compaction. It is vastly reported in the literature, that fibroblasts attach and actively remodel biopolymer hydrogels by synthesizing and reorganizing their fibers and/or chains (44-46). The underlying mechanisms are not yet fully understood, but it was suggested to be related to (i) the forces exerted by the cells during migration or (ii) to the traction exerted by cells presenting significant amounts of contractile proteins (e.g. smooth muscle actin and myosin), or to both mechanisms (47). In the case of this work, the dominant mechanism of the cell-driven compaction is believed to be the first one, since cells are showing a more synthetic rather than contractile phenotype, which will be further discussed in the following sections.

The time effect on the compaction of the gels can also be related with the biodegradable domain comprising by the GTAR sequence in the ELRs specially during the second week of experiment. This motif is sensitive to the urokinase plasminogen activator (uPA enzyme) and therefore is susceptible to be degraded by the HDFn (48). This is supported by the recent publication showing a substantial *in vivo* degradation of a pure hydrogel composed of ELR-RGD and ELR-GTAR after 12 weeks (37). It is worthy to note that, this degradation is expected to be less important in this work since the hydrogel is composed of ELR and collagen, the gel is in contact with just one type of cell and the experiment is carried out in an *in vitro* condition. Furthermore, Figure 2 clearly confirms the presence of ELR all along the experiment and although the thicknesses are visually smaller for the conditions with highest amount of this protein, the dark color is stronger suggesting that the ELRs are more concentrated and they were not just degraded.

The compaction of the collagen matrix has an opposite behavior when insoluble elastin is incorporated in the gel. Ryan, A. J. (2015) showed that the addition of insoluble elastin into collagen gel scaffolds resulted in a resistance to cell-mediated compaction (49). Similarly, Berglund, J. D. et al. (2004) found that scaffolds of collagen gel compacted more than their hybrid

counterparts containing intact elastin (50). The larger structure of insoluble and intact forms of elastin compared to the soluble forms can explain their resistance to cell-mediated compaction.

3.2 Effect of ELR on the cellular metabolic activity

The cell metabolic activity was monitored along the two weeks of experiment to first confirm their viability and to evaluate their proliferation. The metabolic function was expressed in relation to the condition of 0% ELR at Day 1, since pure collagen gel has an inherent biocompatibility (51), which has previously been reported for the reconstituted collagen used in this work (52). Results (Figure 3A) showed no significant difference in the cell metabolic function among all conditions within each time point. An increase in the metabolic function was observed as a function of the progression of the culture, suggesting that the cells were in a favorable environment for their viability and/or proliferation ($p<0.05$ for time and ELR effect, two-way ANOVA).

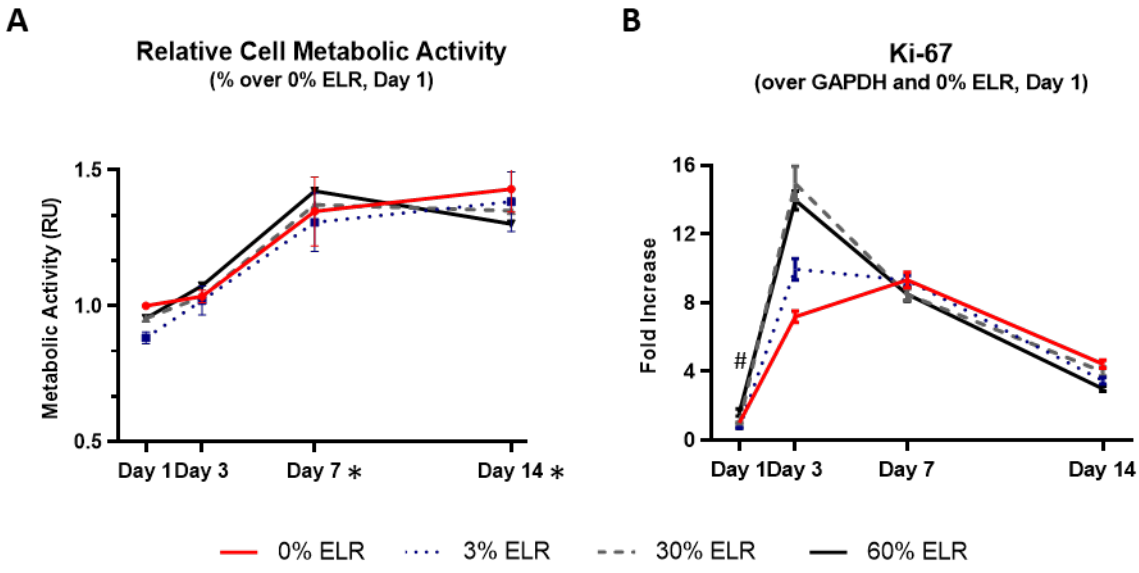

Figure 3: Relative HDFn viability by Alamar Blue Assay and relative proliferation by qRT-PCR. (A) Time course of cell metabolic activity (relative to the condition of 0% ELR at Day 1) and (B) Time course of the ki-67 gene expression (relative to the housekeeping gene and to the condition of 0% ELR at Day 1) for the gels containing 0% (red solid line), 3% (blue round dot line), 30% (gray dash line) and 60% (black solid line) of ELR (n=4, *$p<0.05$ for Day 1 or Day 3 vs Day 7 and Day 14, # $p<0.05$ for 60% ELR vs 0% and 3% ELR).

The Alamar blue assay may not always be directly related to cell proliferation due to a non-linear correlation between dye reduction and cell number that can result to an over-estimation of cell number (53). For this reason, the expression of the gene for the ki-67 protein evaluated by qRT-

PCR was employed as a complementary investigation for cell proliferation. The ki-67 is a suitable cellular marker for this purpose since the protein is present in all active phases of the cell cycle (which the replication of the genetic material occurs) and absent in resting cells (54). Figure 4B shows the results of the gene expression in fold increase in relation to the housekeeping gene GAPDH and to the condition of 0% ELR at Day 1. The presence of ELR in the scaffold stimulated the gene expression in the first days of maturation, achieving 20, 15, and 14-fold increase for the samples containing 60%, 30% and 3% of ELR respectively versus 7-fold increase for the sample without ELR. On the other hand, for Day 7 and Day 14 no statistical difference was found among the conditions. The pronounced expression of the ki-67 gene at Day 3 suggests that the cells were preparing to divide, and this could explain the significant increase from Day 3 to Day 7 in the Alamar Blue results.

The ELR composition used in this work contains the RGD motif, a well-known sequence for cell-adhesion. Testera, A. M. et al (2015) assessed the cytocompatibility of pure ELR gels containing or lacking this bioactive sequence. Alamar Blue tests showed that fibroblasts embedded in ELR gels with the RGD had a sigmoidal growth - slow growth in the first eight days, logarithmic growth between days nine and twelve and stabilization during the last six days of experiment – while fibroblasts in the control gel showed a relatively low and stable signal (41). The growth behavior in this work was similar to the ELR containing the bioactive sequence but shifted to lower time points, which could be explained by the higher cell seeding density that can lead to the earlier growth stabilization.

Cell viability and proliferation were reported to be slightly different with insoluble forms of elastin. Their presence in collagen scaffolds increased SMCs attachment but decreased their proliferation. In addition, gene expression analysis suggested that insoluble elastin modulated SMC phenotype towards a contractile state (49). These findings were in concordance to what previously reported by Mochizuki, S. et al. (2002), who showed that insoluble elastin was responsible for an anti-mitogenic effect in SMCs. This effect might be explained by several overlapping mechanisms, such as masking of growth-factor receptors on the cell surface due to the physical contact with the large particles of insoluble elastin and/or the sequestering of growth factors present in the culture media by the exogenous protein (55).

The same group published that the opposite effect happens with soluble elastin-derived peptides, which have a high affinity to the elastin binding protein receptor (EBP), while showing ability to

trigger transduction of signalling pathways that modulate proliferation of cells (56). Although the biological response is altered in soluble elastin compared to the native insoluble protein towards a more proliferative morphology, this is particularly interesting for tissue engineering purposes since the synthetic state is also responsible for higher ECM production which consequently boost tissue regeneration.

3.2 Effect of ELR on the ECM production by HDFn

The ability of cells to synthesize ECM proteins is crucial to the tissue regeneration and as mentioned, their environment has an important influence on their behavior. The composition of scaffolds has already been showed to modulate cellular response and collagen type I are among the natural polymers that can induce a shift toward a synthetic phenotype (57, 58). The influence of the ELR on the collagenous matrix was analysed by the expression of genes encoding collagen, elastin and fibrilin-1, another important protein involved in the elastic fiber formation. The evaluation of the gene expression rather than the protein itself was chosen to assure that the results were related to the collagen and elastin produced by the cells and not the one added during the fabrication of the samples.

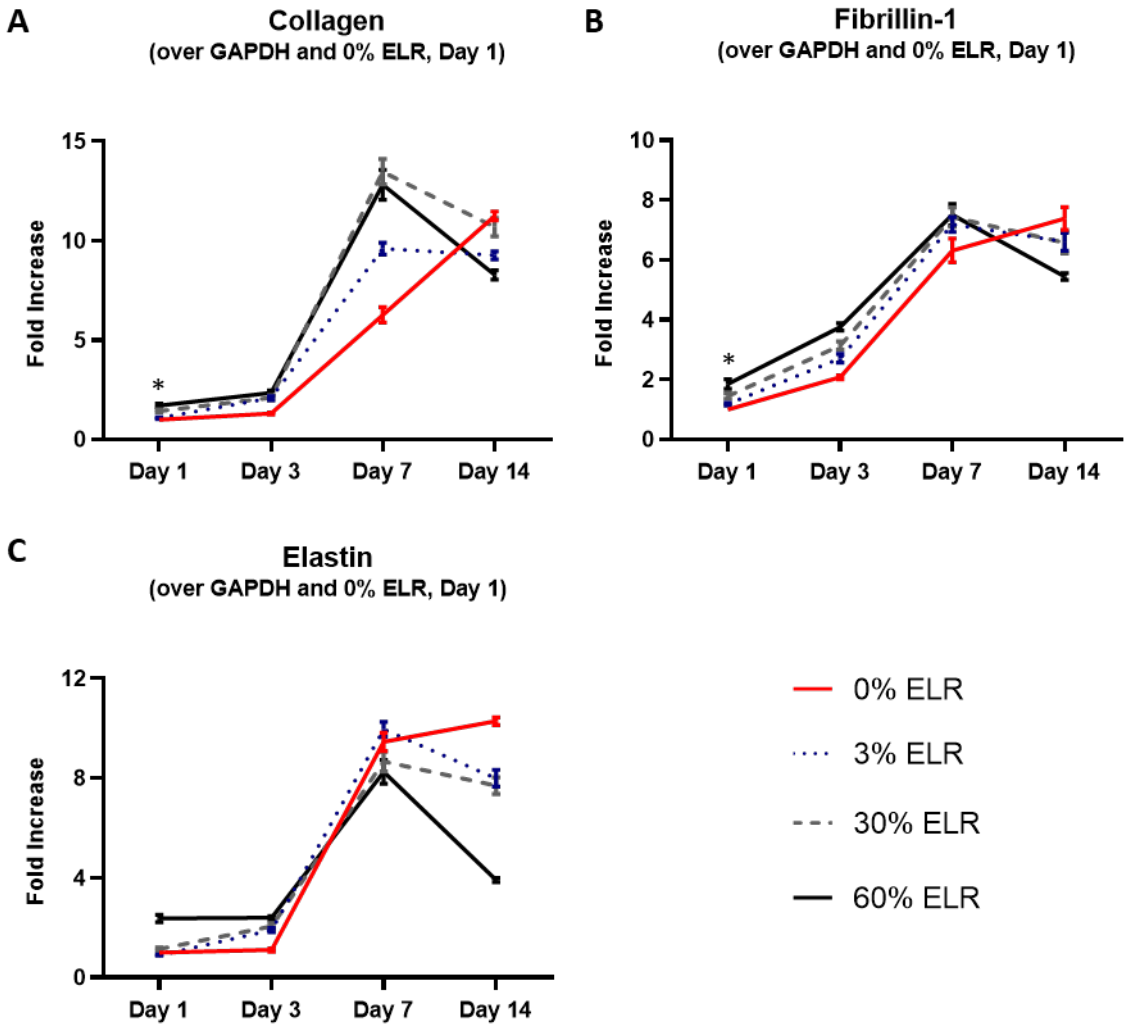

Figure 4: Fold increase in the expression of genes encoding key ECM proteins by qRT-PCR. Time course of the expression of genes encoding (A) collagen, (B) elastin and (C) fibrillin-1 (relative to the housekeeping gene and to the condition of 0% ELR at Day 1) for the gels containing 0% (red solid line), 3% (blue round dot line), 30% (gray dash line) and 60% (black solid line) of ELR (n=3, *p<0.05 for 60% ELR vs 0% and 3% ELR).

Figure 4 shows the results in fold increase over the housekeeping gene GAPDH and the condition of 0% ELR, Day 1. A time dependence on the gene expression was observed during all maturation period ($p<0.05$ for time effect, two-way ANOVA). For collagen (Figure 4A) and fibrilin-1 (Figure 4B), the presence of ELR in the scaffold stimulated their production during the first week ($p<0.05$ for 60% ELR vs 0% and 3% ELR, Day 1, two-way ANOVA). At Day 14, this trend was inversed and the samples containing ELR had a decay in the gene expression suggesting that they are going

towards a more quiescent state. For elastin, the trend was shifted already at Day 7 and the decay was also observed. These results are in accordance with the section 3.2 regarding the more active state of the fibroblasts in presence of ELR specially during the first week of maturation.

Soluble forms of elastin were already showed to be able to trigger a cascade for tissue regeneration. Rnjak, J. et al (2009) showed that a tropoelastin coating promoted the proliferation of HDF compared to collagen coating. The authors also reported that these cells proliferated and expressed extracellular matrix proteins (type I collagen and fibronectin) when seeded in a hydrogel-based scaffold composed of a recombinant human tropoelastin during 14 days of culture (59). Daamen, W. F. et al. (2008) showed that collagen scaffolds containing soluble elastin stimulated the *in vivo* synthesis of elastin, fibrillin-1 and fibrillin-2 when compared to the control (pure collagen) and collagen scaffolds with elastin fibers (60).

A similar upregulation on the expression of ECM proteins by cells was observed in this work in presence of ELR. Complementary, its biodegradable character could have also inferred a synergic effect triggering the ECM remodelling (37). The behavior observed after the first week indicates that the active phase of fibroblasts continues for longer time in the sample without ELR. The results suggest that the different biological cues present in the matrix containing ELR accelerates the maturation leading to an earlier shift to a quiescent phenotype. Although the synthetic state is important for the improvement of the matrix with the newly synthesized ECM proteins, the shift to a quiescent/resting phenotype is also desirable for a functional tissue for a possible application (58).

3.3 Effect of ELR on the gel mechanical properties

An example of the stress response after five cycles of 10% deformation followed by 10 minutes of relaxation is presented in Figure 5A. The data obtained for all samples were well fitted by the chosen model, with R^2 values always higher than 0.9. The initial (Figure 5B) and the equilibrium (Figure 5C) elastic model corresponds to the point right after the deformation and in the end of the relaxation process respectively. The ratio between those two parameters (Figure 5D) shows the predominance of the viscous or elastic component. The strength at break (Figure 5E) and the elongation at break (Figure 5F) correspond to the point of the rupture of the sample. It is worthy to note that, both the collagen and ELR used in this study are different from their physiological structure, so their resulting mechanical properties should not be directly compared with it.

Instead, a careful analysis should be done considering this structural difference, the composition of the conditions and the cell-mediated remodelling that occurs specially in natural scaffolds.

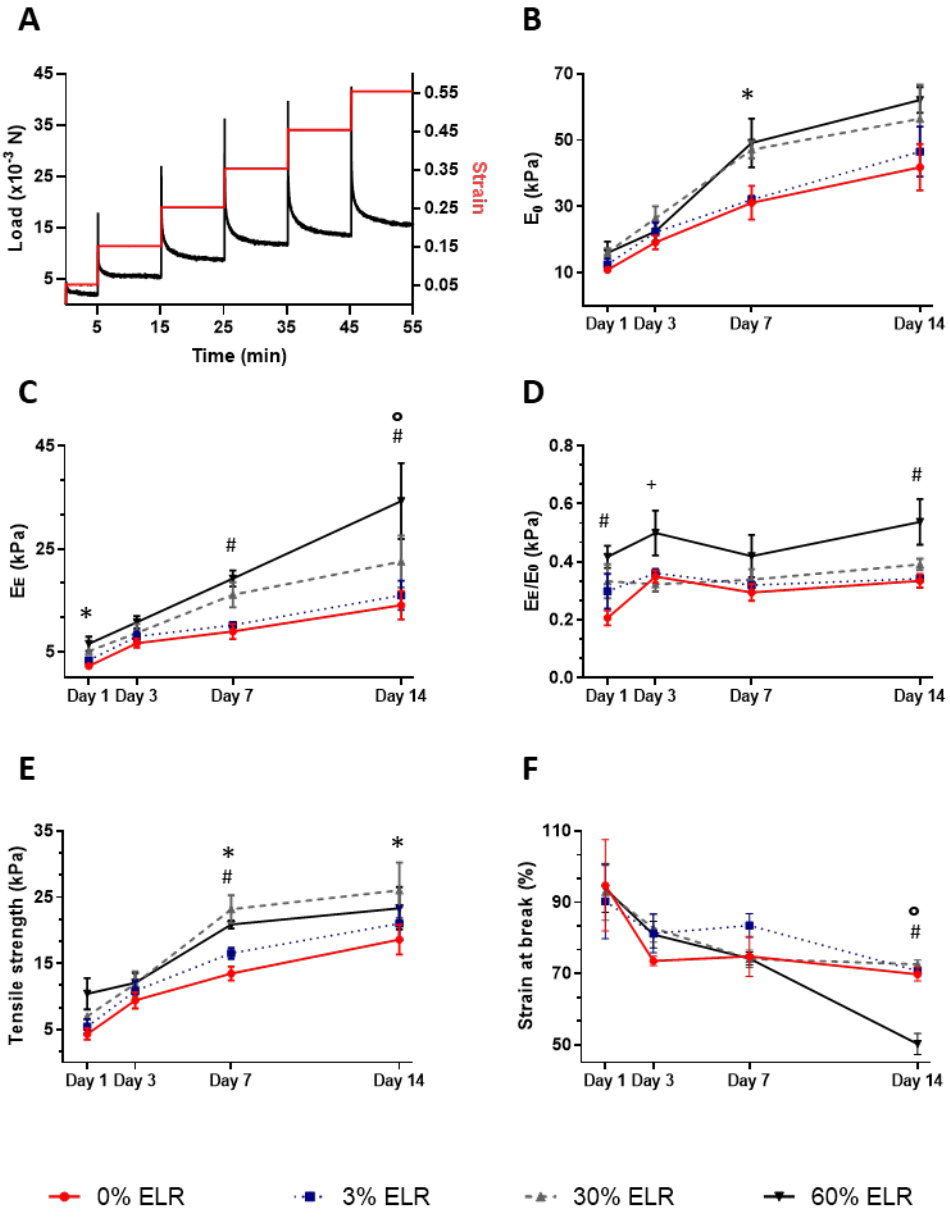

Figure 5: Tensile stress relaxation testing in the circumferential direction of tubular samples. (A) Example of stress-time (black curves) and strain-time (red curves) curves obtained from the progressive tensile stress-relaxation test for the sample containing 30% ELR at Day 7. Time course of (B) tensile initial elastic modulus (E_0), (C) tensile equilibrium elastic modulus (E_E), (D) E_E/E_0 ratio, (E) tensile strength and (F) strain at break for the gels containing 0% (red solid line), 3% (blue

round dot line), 30% (gray dash line) and 60% (black solid line) of ELR (n=4, *p<0.05 for 30% ELR vs 0% and/or 3% ELR, #p<0.05 for 60% ELR vs 0% and/or 3% ELR, ° p<0.05 for 60% ELR vs 30% ELR).

An overall time and ELR concentration dependence on the mechanical properties was observed (p<0.05 for time and ELR effect, two-way ANOVA). At Day 1, the presence of the ELR improved the elastic modulus and strength of the gels. Although the strongest compaction occurred already at this time point, this process is likely to be mainly related to the mechanisms of gel formation rather than cell remodelling. Therefore, the mechanical results predominantly reflect the influence of ELR in the collagenous matrix. Comparing the ratio between the elastic modulus, the viscous part is less evident in the samples containing ELR which can be a result of its lower water content presumably assigned to the elastin hydrophobic character. The strain at failure was not influenced by the addition of the polymer.

After three days of maturation, the effect of cell attachment, migration and remodelling should already be considered on the resulting mechanical properties and this influence may be related to the approximation of the elastic modulus and strength values. Indeed, for this time point no statistical difference was found (p<0.05, two-way ANOVA). The mechanical reinforcement along the first week for all conditions can be mainly attributed to the expression of ECM components by the cells. As it was mentioned in the previous sections, the presence of ELR seemed to increase the expression of genes encoding key ECM proteins which could explain the differences in the elastic modulus and tensile strength at Day 7 among the conditions (p<0.05 for 30% and/or 60% ELR vs 0% and/or 3% ELR, two-way ANOVA). Particularly for the tensile strength, the sample containing 30% ELR reached the one containing 60% ELR.

The elastic modulus continued to be directly related to the amount of ELR, i.e. highest values for the conditions with highest amount of ELR. The ratio between the elastic modulus for the sample of 60% ELR were always above the other conditions. The relative strong increase in the E_E for this condition at Day 14 (and consequently increase in the ratio E_E/E_0) suggests that the viscous component is becoming less representative and the maturation time is orienting the sample towards a pure elastic behavior. At the same time, the strain at break suffered a strong decrease from 74% to 50% in the second week, while the other conditions remained around 70%.

The key function of elastin and rubber-like proteins in the body is to provide low stiffness, high strain and efficient elastic-energy storage components in tissues (61). As mentioned before, the

correlation of the mechanical behavior of native and other forms of elastin is not straightforward. For the insoluble forms of elastin incorporated in collagen scaffolds, it was observed a reduction in the scaffold stiffness due to the decrease of both compressive and tensile modulus in a concentration dependent manner (49). On the other hand, a cellularized hybrid construct (intact elastin scaffolds with collagen gel) was reported to have higher burst strength, initial and equilibrium elastic modulus than control collagen gel (50).

In this work, the incorporation of 30% ELR into collagen gel increased the initial elastic modulus by 33%, the equilibrium elastic modulus by 64% and the tensile strength by 37% without compromising its strain at failure. For this reason, this sample is able to absorb more energy before breaking and consequently more energy in the elastic region. In addition, the viscous and the elastic behavior remains similar during the maturation time, approaching the ratio of ca. 0.33 reported in literature for coronary artery (50). Therefore, this combination of elastin and collagen was found beneficial for the development of cellularized tubular constructs for vascular tissue engineering applications. Interestingly, this is the same elastin/collagen proportion found in saphenous veins, the standard autologous grafts in bypass surgeries (62).

The strength at break achieved by this condition at the end of the second week of the experiment was equal to 26 kPa. The circumferential yield stress for human coronary and internal mammary arteries (internal diameter between 2-3 mm) was reported to be close to 100 kPa (63). This value corresponds to a point close to the limit of the elastic regime and so it is located slightly below the stress at break. The introduction of ELR improved the strength of cellularized collagen gel-based constructs, however, different strategies still need to be combined to further improve its mechanical properties towards physiological values. The employed collagen and ELR concentration (27, 64), the selected crosslinkable motifs (65, 66) and/or the introduction of self-assembling domains in the ELR, such as silk (29, 67) or leucine zipper sequences (30, 68) can be explored to reinforce the matrix. In addition, the synthesis of ECM proteins by the cells could be boosted by increasing the cell seeding density (69) or by introducing a dynamic stimulation in a perfusion bioreactor (70).

4 Conclusion

The increasing concentration of ELR in the composite gel enhanced construct compaction already after one day of maturation due to the hydrophobic character of the molecule. The continuous compaction during the time are predominantly related to cell-mediated remodelling. The

degradable motif present in one of the ELR version (ELR-GTAR) could also have had an influence on this process even if in lower scale. The introduction of the ELR in the known biocompatible collagen matrix did not change the cell viability. However, their proliferation was enhanced in the first week of maturation which can be related to the presence of the protein itself and to the RGD motifs included on them. Similarly, the expression of genes encoding collagen, elastin, fibrillin-1 was upregulated. Overall, the results obtained in this work are aligned to those present in literature using soluble forms of elastin. The suggested phenotypic shift towards a more synthetic state in this case are beneficial for tissue regeneration. This synthetic state and the presence of the ELR itself are believed to be related with the increase in the initial and equilibrium elastic modulus and the tensile strength of the constructs. Altogether, this works suggests the use of 30% ELR/collagen (mass ratio) for the production of cellularized tubular gel constructs since this condition benefit from the mentioned improvement without compromising the strain at break. The versatile character of ELRs is a key advantage of this approach and further investigation on the crosslinking technology and the design of modular versions encompassing self-assembling protein-based sequences can be envisaged to enhance the mechanical properties of the constructs. Alternative strategies such as increasing polymer concentration, increasing cell seeding density and applying a dynamic stimulation during maturation can also contribute to this goal towards a physiological performance.

5 Acknowledgements

This work was partially supported by the Natural Sciences and Engineering Research Council of Canada (NSERC), the NSERC Create Program in Regenerative Medicine, the Canadian Foundation for the Innovation, the Fonds de Recherche du Québec (Nature et Technologies, and Santé), the Spanish Government (MAT2016-78903-R, RTI2018-096320-B-C22, FPU15-00448), Junta de Castilla y León (VA317P18), Interreg V A España Portugal POCTEP (0624_2IQBIONEURO_6_E) and Centro en Red de Medicina Regenerativa y Terapia Celular de Castilla y León.

6 References

1. Cen L, Liu W, Cui L, Zhang W, Cao Y. Collagen tissue engineering: development of novel biomaterials and applications. Pediatric research. 2008;63(5):492.
2. Glowacki J, Mizuno S. Collagen scaffolds for tissue engineering. Biopolymers: Original Research on Biomolecules. 2008;89(5):338-44.
3. Parenteau-Bareil R, Gauvin R, Berthod F. Collagen-based biomaterials for tissue engineering applications. Materials. 2010;3(3):1863-87.
4. Daamen WF, Veerkamp J, Van Hest J, Van Kuppevelt T. Elastin as a biomaterial for tissue engineering. Biomaterials. 2007;28(30):4378-98.

5. Kim I-Y, Seo S-J, Moon H-S, Yoo M-K, Park I-Y, Kim B-C, et al. Chitosan and its derivatives for tissue engineering applications. Biotechnology advances. 2008;26(1):1-21.
6. Ahmed TAE, Dare EV, Hincke M. Fibrin: A Versatile Scaffold for Tissue Engineering Applications. Tissue Engineering Part B: Reviews. 2008;14(2):199-215.
7. Loy C, Meghezi S, Levesque L, Pezzoli D, Kumra H, Reinhardt D, et al. A planar model of the vessel wall from cellularized-collagen scaffolds: focus on cell-matrix interactions in mono-,bi- and tri-culture models. Biomaterials Science. 2017;5(1):153-62.
8. Loy C, Pezzoli D, Candiani G, Mantovani D. A Cost-Effective Culture System for the In Vitro Assembly, Maturation, and Stimulation of Advanced Multilayered Multiculture Tubular Tissue Models. Biotechnology Journal. 2017;, in press.
9. Aya R, Ishiko T, Noda K, Yamawaki S, Sakamoto Y, Tomihata K, et al. Regeneration of elastic fibers by three-dimensional culture on a collagen scaffold and the addition of latent TGF-β binding protein 4 to improve elastic matrix deposition. Biomaterials. 2015;72:29-37.
10. Lee K-W, Stolz DB, Wang Y. Substantial expression of mature elastin in arterial constructs. Proceedings of the National Academy of Sciences. 2011;108(7):2705-10.
11. Lin S, Sandig M, Mequanint K. Three-Dimensional Topography of Synthetic Scaffolds Induces Elastin Synthesis by Human Coronary Artery Smooth Muscle Cells. Tissue Engineering Part A. 2011;17(11-12):1561-71.
12. Venkataraman L, Bashur CA, Ramamurth A. Impact of Cyclic Stretch on Induced Elastogenesis Within Collagenous Conduits. Tissue Engineering Part A. 2014;20(9-10):1403-15.
13. Hinderer S, Shen N, Ringuette L-J, Hansmann J, Reinhardt DP, Brucker SY, et al. In vitro elastogenesis: instructing human vascular smooth muscle cells to generate an elastic fiber-containing extracellular matrix scaffold. Biomedical Materials. 2015;10(3):034102.
14. Venkataraman L, Ramamurthi A. Induced elastic matrix deposition within three-dimensional collagen scaffolds. Tissue Engineering part A. 2011;17(21-22):2879-89.
15. Almine JF, Bax DV, Mithieux SM, Nivison-Smith L, Rnjak J, Waterhouse A, et al. Elastin-based materials. Chemical Society Reviews. 2010;39(9):3371-9.
16. Mithieux SM, Wise SG, Weiss AS. Tropoelastin—A multifaceted naturally smart material. Advanced drug delivery reviews. 2013;65(4):421-8.
17. Kim W, Chaikof EL. Recombinant elastin-mimetic biomaterials: Emerging applications in medicine. Advanced Drug Delivery Reviews. 2010;62(15):1468-78.
18. Sengupta D, Heilshorn SC. Protein-engineered biomaterials: highly tunable tissue engineering scaffolds. Tissue Engineering Part B: Reviews. 2010;16(3):285-93.
19. Girotti A, Fernández-Colino A, López IM, Rodríguez-Cabello JC, Arias FJ. Elastin-like recombinamers: Biosynthetic strategies and biotechnological applications. Biotechnology journal. 2011;6(10):1174-86.
20. Nettles DL, Chilkoti A, Setton LA. Applications of elastin-like polypeptides in tissue engineering. Advanced Drug Delivery Reviews. 2010;62(15):1479-85.
21. Nivison-Smith L, Rnjak J, Weiss AS. Synthetic human elastin microfibers: stable cross-linked tropoelastin and cell interactive constructs for tissue engineering applications. Acta biomaterialia. 2010;6(2):354-9.
22. Putzu M, Causa F, Nele V, de Torre IG, Rodriguez-Cabello J, Netti P. Elastin-like-recombinamers multilayered nanofibrous scaffolds for cardiovascular applications. Biofabrication. 2016;8(4):045009.
23. de Torre IG, Ibáñez-Fonseca A, Quintanilla L, Alonso M, Rodríguez-Cabello J-C. Random and oriented electrospun fibers based on a multicomponent, in situ clickable elastin-like recombinamer system for dermal tissue engineering. Acta biomaterialia. 2018;72:137-49.

24. Welsh ER, Tirrell DA. Engineering the extracellular matrix: a novel approach to polymeric biomaterials. I. Control of the physical properties of artificial protein matrices designed to support adhesion of vascular endothelial cells. Biomacromolecules. 2000;1(1):23-30.
25. Liu JC, Heilshorn SC, Tirrell DA. Comparative cell response to artificial extracellular matrix proteins containing the RGD and CS5 cell-binding domains. Biomacromolecules. 2004;5(2):497-504.
26. Heilshorn SC, Liu JC, Tirrell DA. Cell-binding domain context affects cell behavior on engineered proteins. Biomacromolecules. 2005;6(1):318-23.
27. de Torre IG, Santos M, Quintanilla L, Testera A, Alonso M, Cabello JCR. Elastin-like recombinamer catalyst-free click gels: characterization of poroelastic and intrinsic viscoelastic properties. Acta biomaterialia. 2014;10(6):2495-505.
28. Trabbic-Carlson K, Setton LA, Chilkoti A. Swelling and mechanical behaviors of chemically cross-linked hydrogels of elastin-like polypeptides. Biomacromolecules. 2003;4(3):572-80.
29. Fernández-Colino A, Arias FJ, Alonso M, Rodríguez-Cabello JC. Self-organized ECM-mimetic model based on an amphiphilic multiblock silk-elastin-like corecombinamer with a concomitant dual physical gelation process. Biomacromolecules. 2014;15(10):3781-93.
30. Fernández-Colino A, Arias FJ, Alonso M, Rodríguez-Cabello JC. Amphiphilic elastin-like block co-recombinamers containing leucine zippers: Cooperative interplay between both domains results in injectable and stable hydrogels. Biomacromolecules. 2015;16(10):3389-98.
31. McKenna KA, Hinds MT, Sarao RC, Wu P-C, Maslen CL, Glanville RW, et al. Mechanical property characterization of electrospun recombinant human tropoelastin for vascular graft biomaterials. Acta biomaterialia. 2012;8(1):225-33.
32. Di Zio K, Tirrell DA. Mechanical properties of artificial protein matrices engineered for control of cell and tissue behavior. Macromolecules. 2003;36(5):1553-8.
33. Girotti A, Reguera J, Rodríguez-Cabello JC, Arias FJ, Alonso M, Testera AM. Design and bioproduction of a recombinant multi (bio) functional elastin-like protein polymer containing cell adhesion sequences for tissue engineering purposes. Journal of Materials Science: Materials in Medicine. 2004;15(4):479-84.
34. Sommar P, Pettersson S, Ness C, Johnson H, Kratz G, Junker JP. Engineering three-dimensional cartilage-and bone-like tissues using human dermal fibroblasts and macroporous gelatine microcarriers. Journal of Plastic, Reconstructive & Aesthetic Surgery. 2010;63(6):1036-46.
35. Costa-Almeida R, Soares R, Granja PL. Fibroblasts as maestros orchestrating tissue regeneration. Journal of tissue engineering and regenerative medicine. 2018;12(1):240-51.
36. Bourget J-M, Gauvin R, Larouche D, Lavoie A, Labbé R, Auger FA, et al. Human fibroblast-derived ECM as a scaffold for vascular tissue engineering. Biomaterials. 2012;33(36):9205-13.
37. Flora T, de Torre IG, Alonso M, Rodríguez-Cabello JC. Use of proteolytic sequences with different cleavage kinetics as a way to generate hydrogels with preprogrammed cell-infiltration patterns imparted over their given 3D spatial structure. Biofabrication. 2019;11(3):035008.
38. Shu XZ, Ghosh K, Liu Y, Palumbo FS, Luo Y, Clark RA, et al. Attachment and spreading of fibroblasts on an RGD peptide–modified injectable hyaluronan hydrogel. Journal of Biomedical Materials Research Part A: An Official Journal of The Society for Biomaterials, The Japanese Society for Biomaterials, and The Australian Society for Biomaterials and the Korean Society for Biomaterials. 2004;68(2):365-75.
39. Rodríguez-Cabello JC, Girotti A, Ribeiro A, Arias FJ. Synthesis of genetically engineered protein polymers (recombinamers) as an example of advanced self-assembled smart materials. Nanotechnology in Regenerative Medicine: Springer; 2012. p. 17-38.

40. Rajan N, Habermehl J, Cote M-F, Doillon CJ, Mantovani D. Preparation of ready-to-use, storable and reconstituted type I collagen from rat tail tendon for tissue engineering applications. Nat Protocols. 2007;1(6):2753-8.
41. Testera AM, Girotti A, de Torre IG, Quintanilla L, Santos M, Alonso M, et al. Biocompatible elastin-like click gels: design, synthesis and characterization. Journal of Materials Science: Materials in Medicine. 2015;26(2):105.
42. Meghezi S, Seifu DG, Bono N, Unsworth L, Mequanint K, Mantovani D. Engineering 3D Cellularized Collagen Gels for Vascular Tissue Regeneration. Jove-Journal of Visualized Experiments. 2015(100):52812.
43. Meghezi S, Couet F, Chevallier P, Mantovani D. Effects of a Pseudophysiological Environment on the Elastic and Viscoelastic Properties of Collagen Gels. International Journal of Biomaterials. 2012;2012:Article ID 319290.
44. Eastwood M, Porter R, Khan U, McGrouther G, Brown R. Quantitative analysis of collagen gel contractile forces generated by dermal fibroblasts and the relationship to cell morphology. Journal of cellular physiology. 1996;166(1):33-42.
45. Andujar M, Melin M, Guerret S, Grimaud J. Cell migration influences collagen gel contraction. Journal of submicroscopic cytology and pathology. 1992;24(2):145-54.
46. Kanekar S, Borg TK, Terracio L, Carver W. Modulation of heart fibroblast migration and collagen gel contraction by IGF-I. Cell adhesion and communication. 2000;7(6):513-23.
47. Shreiber DI, Barocas VH, Tranquillo RT. Temporal variations in cell migration and traction during fibroblast-mediated gel compaction. Biophysical journal. 2003;84(6):4102-14.
48. Vassalli J-D, Sappino A, Belin D. The plasminogen activator/plasmin system. The Journal of clinical investigation. 1991;88(4):1067-72.
49. Ryan AJ, O'Brien FJ. Insoluble elastin reduces collagen scaffold stiffness, improves viscoelastic properties, and induces a contractile phenotype in smooth muscle cells. Biomaterials. 2015;73:296-307.
50. Berglund JD, Nerem RM, Sambanis A. Incorporation of intact elastin scaffolds in tissue-engineered collagen-based vascular grafts. Tissue Engineering. 2004;10(9-10):1526-35.
51. Bonnier F, Keating M, Wrobel TP, Majzner K, Baranska M, Garcia-Munoz A, et al. Cell viability assessment using the Alamar blue assay: a comparison of 2D and 3D cell culture models. Toxicology in vitro. 2015;29(1):124-31.
52. Copes F, Chevallier P, Loy C, Pezzoli D, Boccafoschi F, Mantovani D. Heparin-modified Collagen gels for controlled release of Pleiotrophin: Potential for vascular applications. Frontiers in bioengineering and biotechnology. 2019;7:74.
53. Rampersad SN. Multiple applications of Alamar Blue as an indicator of metabolic function and cellular health in cell viability bioassays. Sensors. 2012;12(9):12347-60.
54. Scholzen T, Gerdes J. The Ki-67 protein: from the known and the unknown. Journal of cellular physiology. 2000;182(3):311-22.
55. Urbán Z, Riazi S, Seidl TL, Katahira J, Smoot LB, Chitayat D, et al. Connection between Elastin Haploinsufficiency and Increased Cell Proliferation in Patients with Supravalvular Aortic Stenosis and Williams-Beuren Syndrome. The American Journal of Human Genetics. 2002;71(1):30-44.
56. Mochizuki S, Brassart B, Hinek A. Signaling pathways transduced through the elastin receptor facilitate proliferation of arterial smooth muscle cells. Journal of Biological Chemistry. 2002;277(47):44854-63.
57. Grinnell F. Fibroblast biology in three-dimensional collagen matrices. Trends in cell biology. 2003;13(5):264-9.

58. Chan-Park MB, Shen JY, Cao Y, Xiong Y, Liu Y, Rayatpisheh S, et al. Biomimetic control of vascular smooth muscle cell morphology and phenotype for functional tissue-engineered small-diameter blood vessels. Journal of Biomedical Materials Research Part A: An Official Journal of The Society for Biomaterials, The Japanese Society for Biomaterials, and The Australian Society for Biomaterials and the Korean Society for Biomaterials. 2009;88(4):1104-21.
59. Rnjak J, Li Z, Maitz PK, Wise SG, Weiss AS. Primary human dermal fibroblast interactions with open weave three-dimensional scaffolds prepared from synthetic human elastin. Biomaterials. 2009;30(32):6469-77.
60. Daamen WF, Nillesen ST, Wismans RG, Reinhardt DP, Hafmans T, Veerkamp JH, et al. A biomaterial composed of collagen and solubilized elastin enhances angiogenesis and elastic fiber formation without calcification. Tissue Engineering Part A. 2008;14(3):349-60.
61. Gosline J, Lillie M, Carrington E, Guerette P, Ortlepp C, Savage K. Elastic proteins: biological roles and mechanical properties. Philosophical Transactions of the Royal Society B: Biological Sciences. 2002;357(1418):121.
62. Venturi M, Bonavina L, Annoni F, Colombo L, Butera C, Peracchia A, et al. Biochemical assay of collagen and elastin in the normal and varicose vein wall. Journal of Surgical Research. 1996;60(1):245-8.
63. Van Andel CJ, Pistecky PV, Borst C. Mechanical properties of porcine and human arteries: implications for coronary anastomotic connectors. The Annals of thoracic surgery. 2003;76(1):58-64.
64. Tierney CM, Haugh MG, Liedl J, Mulcahy F, Hayes B, O'Brien FJ. The effects of collagen concentration and crosslink density on the biological, structural and mechanical properties of collagen-GAG scaffolds for bone tissue engineering. Journal of the mechanical behavior of biomedical materials. 2009;2(2):202-9.
65. Krishna UM, Martinez AW, Caves JM, Chaikof EL. Hydrazone self-crosslinking of multiphase elastin-like block copolymer networks. Acta biomaterialia. 2012;8(3):988-97.
66. Madl CM, Katz LM, Heilshorn SC. Bio-Orthogonally Crosslinked, Engineered Protein Hydrogels with Tunable Mechanics and Biochemistry for Cell Encapsulation. Advanced functional materials. 2016;26(21):3612-20.
67. Huang W, Tarakanova A, Dinjaski N, Wang Q, Xia X, Chen Y, et al. Design of Multistimuli Responsive Hydrogels Using Integrated Modeling and Genetically Engineered Silk–Elastin-Like Proteins. Advanced functional materials. 2016;26(23):4113-23.
68. Salinas-Fernández S, Santos M, Alonso M, Quintanilla L, Rodríguez-Cabello JC. Genetically engineered elastin-like recombinamers with sequence-based molecular stabilization as advanced bioinks for 3D bioprinting. Applied Materials Today. 2019:100500.
69. Camasão DB, Pezzoli D, Loy C, Kumra H, Levesque L, Reinhardt DP, et al. Increasing Cell Seeding Density Improves Elastin Expression and Mechanical Properties in Collagen Gel-Based Scaffolds Cellularized with Smooth Muscle Cells. Biotechnology Journal. 2018;0(0):1700768.
70. Huang AH, Balestrini JL, Udelsman BV, Zhou KC, Zhao L, Ferruzzi J, et al. Biaxial stretch improves elastic fiber maturation, collagen arrangement, and mechanical properties in engineered arteries. Tissue Engineering Part C: Methods. 2016;22(6):524-33.